iScience, Volume *26*

Supplemental information

Eliminating host-guest incompatibility via enzyme mining enables the high-temperature production of *N*-acetylglucosamine

Yutong Wu, Jiongqin Liu, Xiao Han, Xuanlin Meng, Mengke Li, Jing Wang, Hongsong Xue, Yuhan Yang, Ping Xu, and Fei Tao

Supplemental Information

Supplementary Figures

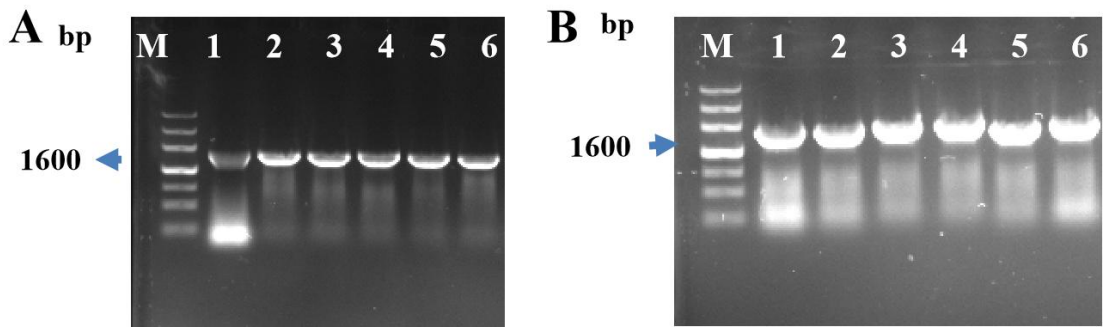

Figure S1. Analysis of the constructed plasmids by restriction enzyme digestion, related to Figure 3.

(A) M, marker; 1-3 analysis of pKVMΔ*gamA*; 4-6 analysis of pKVMΔ*nagAB*

(B) M, marker; 1-3 analysis of pKVMΔ*nagP1*; 4-6 analysis of pKVMΔ*nagP2*

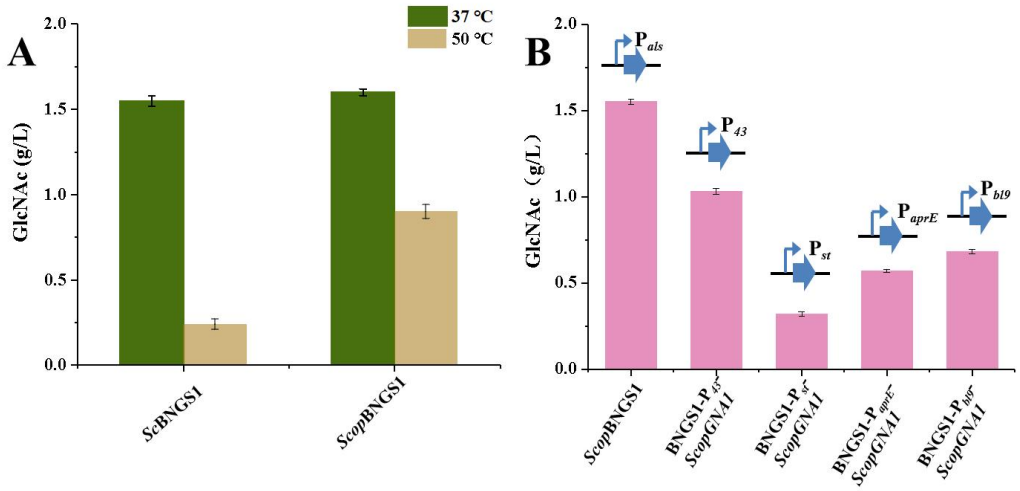

Figure S2. Codon optimization and promoter screening, related to Figure 3.

(A) Shake flask fermentation of *Sc*BNGS1 and *Scop*BNGS1 at 37℃ and 50℃.

(B) Different promoter screening at 37℃.

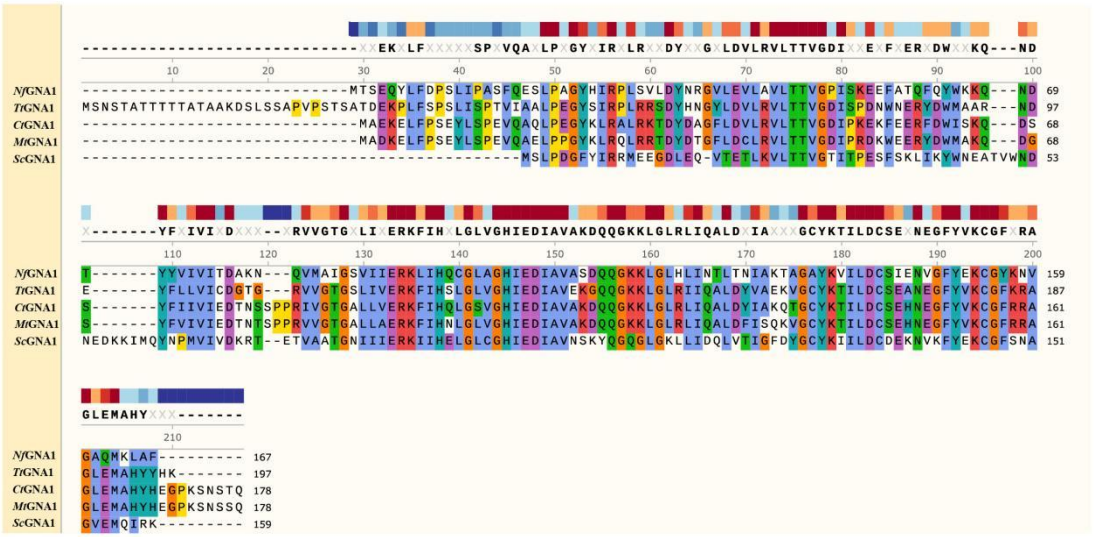

Figure S3. Multiple alignment of *Sc*GNA1 with *Tt*GNA1, *Ct*GNA1, *Mt*GNA1, and *Nf*GNA1, related to Figure 2, Figure 3 and Figure 4.

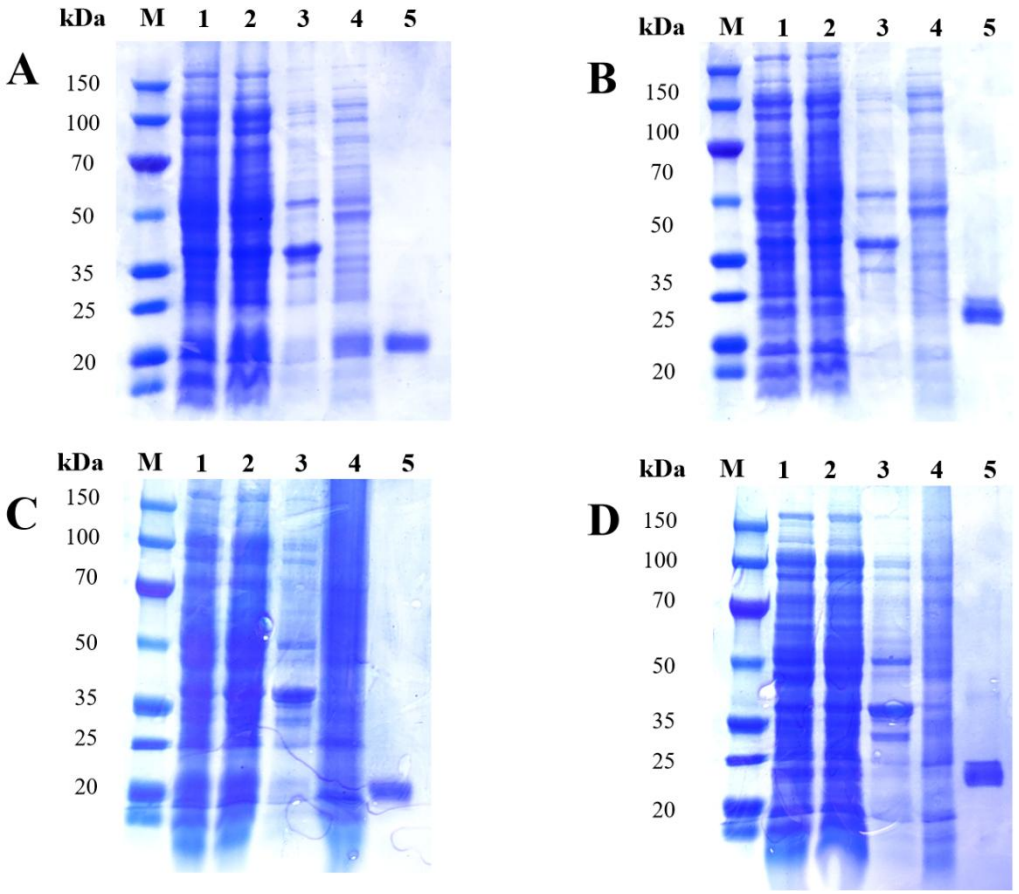

Figure S4. Purification of *Tt*GNA1, *Ct*GNA1, *Mt*GNA1, and *Nf*GNA1, related to Figure 4.

(A) SDS-PAGE of purified *Nf*GNA1. Lane M, marker; lane 1, cell disruption solution of *Nf*GNA1; lane 2, precipitation of induced cell lysate; lane 3, supernatant of induced cell lysate; lane 4, Elute *Nf*GNA1 with 50mM imidazole; lane 5, Elute *Nf*GNA1 with 200mM imidazole.

(B) SDS-PAGE of purified *Ct*GNA1. Lane M, marker; lane 1, cell disruption solution of *Ct*GNA1; lane 2, precipitation of induced cell lysate; lane 3, supernatant of induced cell lysate; lane 4, Elute *Ct*GNA1 with 50mM imidazole; lane 5, Elute *Ct*GNA1 with 200mM imidazole.

(C) SDS-PAGE of purified *Mt*GNA1. Lane M, marker; lane 1, cell disruption solution of *Mt*GNA1; lane 2, precipitation of induced cell lysate; lane 3, supernatant of induced cell lysate; lane 4, Elute *Mt*GNA1 with 50mM imidazole; lane 5, Elute *Mt*GNA1 with 200mM imidazole.

(D) Elute *Tt*GNA1 with 200mM imidazole; lane 6, cell disruption solution of *Tt*GNA1; lane 7, precipitation of induced cell lysate; lane 8, supernatant of induced cell lysate; lane 4, Elute *Tt*GNA1 with 50mM imidazole; lane 5, Elute *Tt*GNA1 with 200mM imidazole.

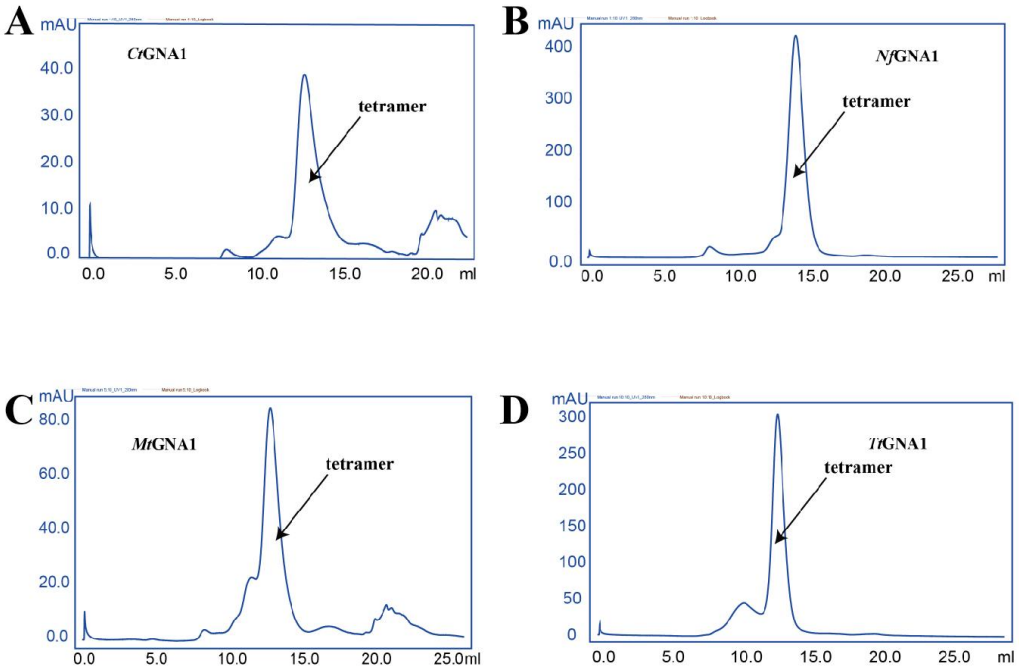

Figure S5. Analysis of size exclusion chromatography on Superdex 200 (ÄTKA purifier) of *Ct*GNA1, *Nf*GNA1, *Mt*GNA1, and *Tt*GNA1, related to Figure 4 and Figure 5.

Each of the elution volume of *Ct*GNA1, *Nf*GNA1, *Mt*GNA1, and *Tt*GNA1 is 13.7 mL, 14 mL, 13.7 mL and 13.6 mL, respectively. The equations for the molecular masses of the standard proteins were used versus their elution volume values: y = –0.31427x + 1.89014, x = lg Mr, y = Kav (Ve-Vo)/(Vc-Vo).

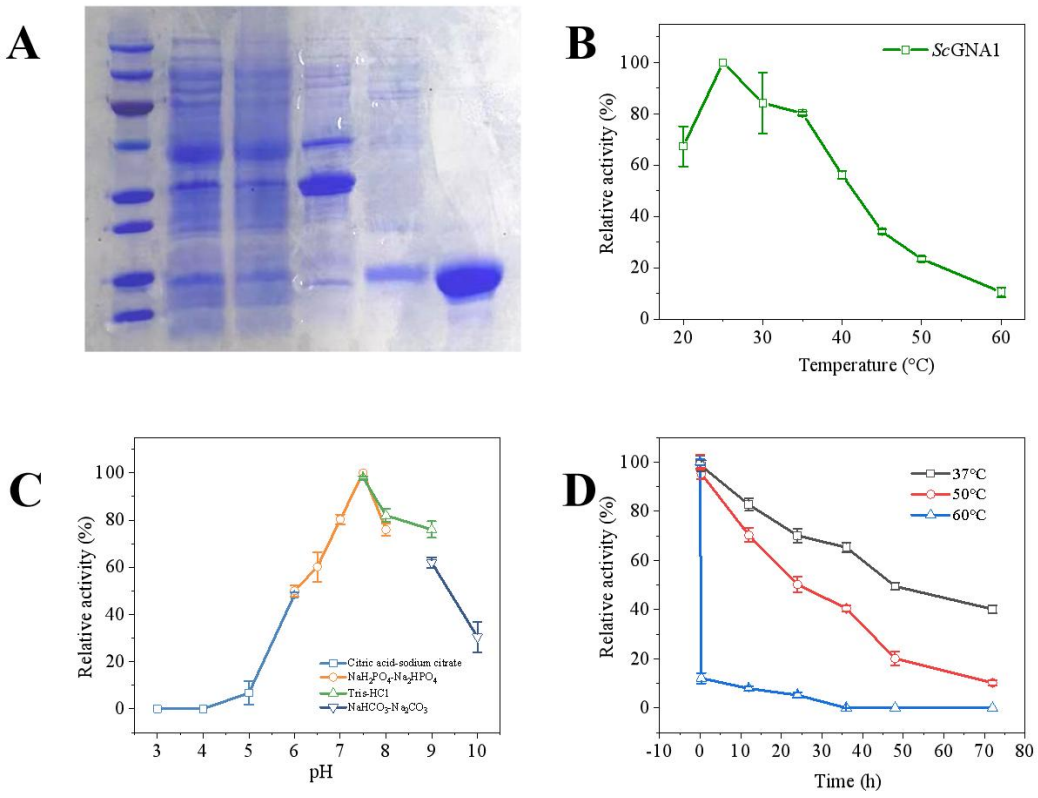

Figure S6. Activity assay of *Sc*GNA1, related to Figure 4.

(A) SDS-PAGE of purified *Sc*GNA1. Lane M, marker; lane 1, cell disruption solution of *Sc*GNA1; lane 2, precipitation of induced cell lysate; lane 3, supernatant of induced cell lysate; lane 4, Elute *Sc*GNA1 with 50mM imidazole; lane 5, Elute *Sc*GNA1 with 200mM imidazole.

(B) Effects of temperature on the activities of *Sc*GNA1.

(C) Effects of pH on activities of *Sc*GNA1. Square, citric acid-sodium citrate; Triangle, NaH_2PO_4-Na_2HPO_4; Rhombus, Tris-HCl; Star, $NaHCO_3$-Na_2CO_3.

(D) Thermal stability of *Sc*GNA1 at 37°C, 50°C, and 60°C.

Triplicate experiments were carried out for physiological measurements, and error bars represent standard deviation.

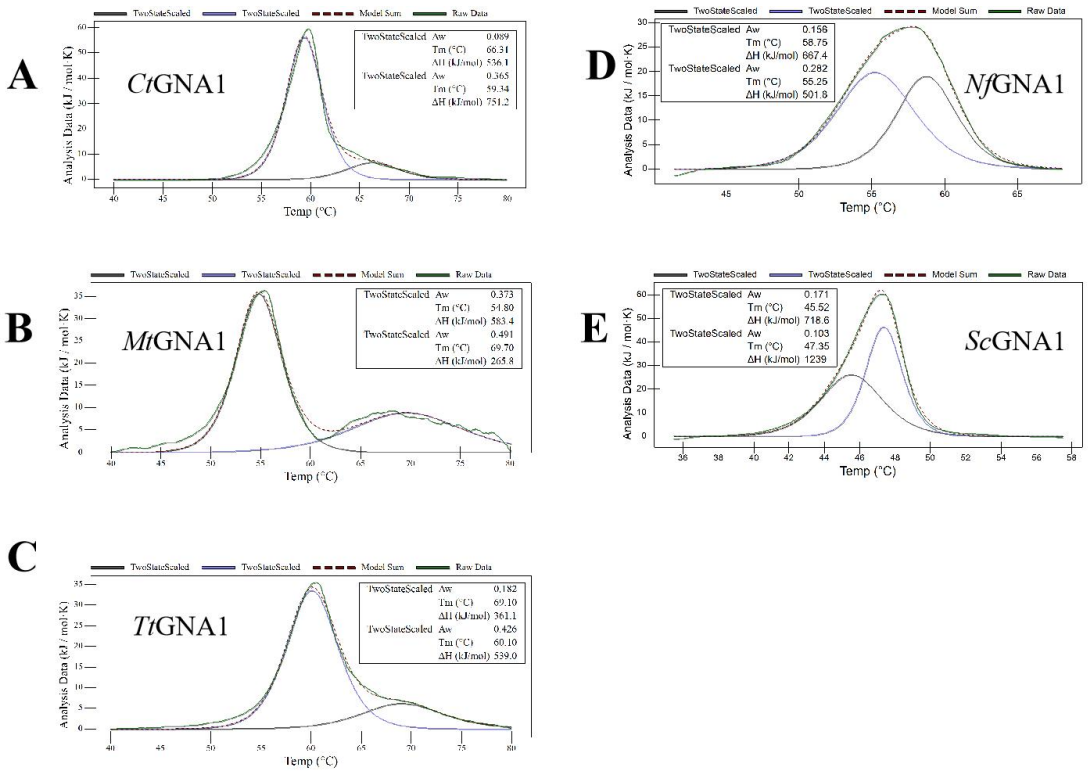

Figure S7. Protein thermostability tests for *Ct*GNA1, *Mt*GNA1, *Tt*GNA1, *Nf*GNA1, and *Sc*GNA1 using nano differential scanning calorimeter (Nano DSC, the TA instruments, USA), related to Figure 4.

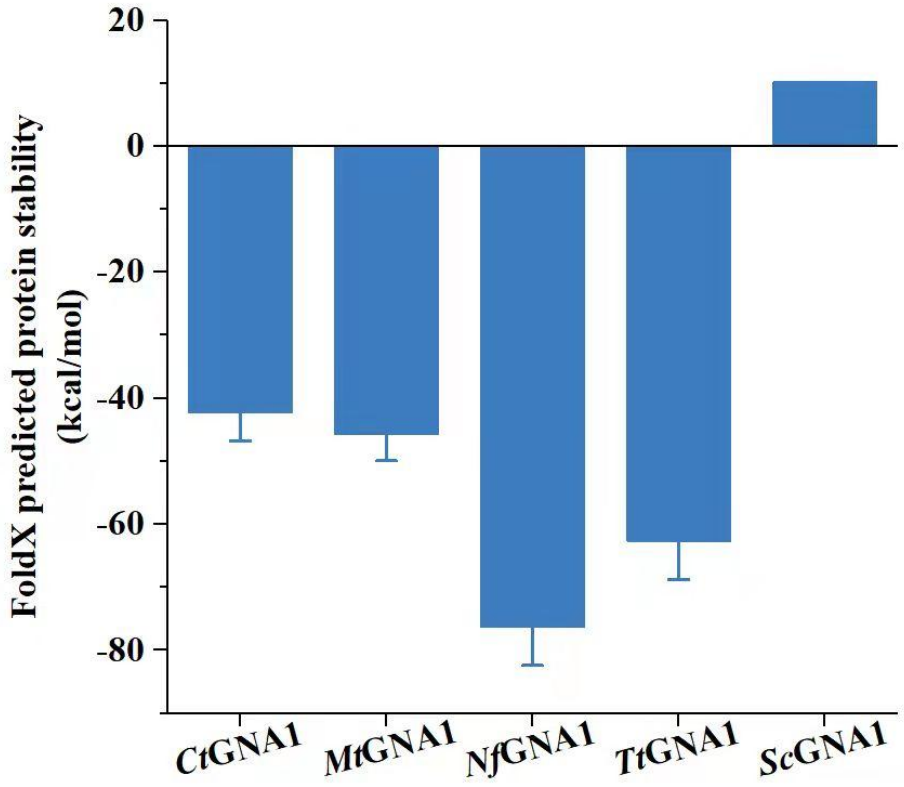

Figure S8. Protein stability prediction of *Tt*GNA1, *Mt*GNA1, *Nf*GNA1, *Ct*GNA1, and *Sc*GNA1 based on FoldX, related to Figure 5.

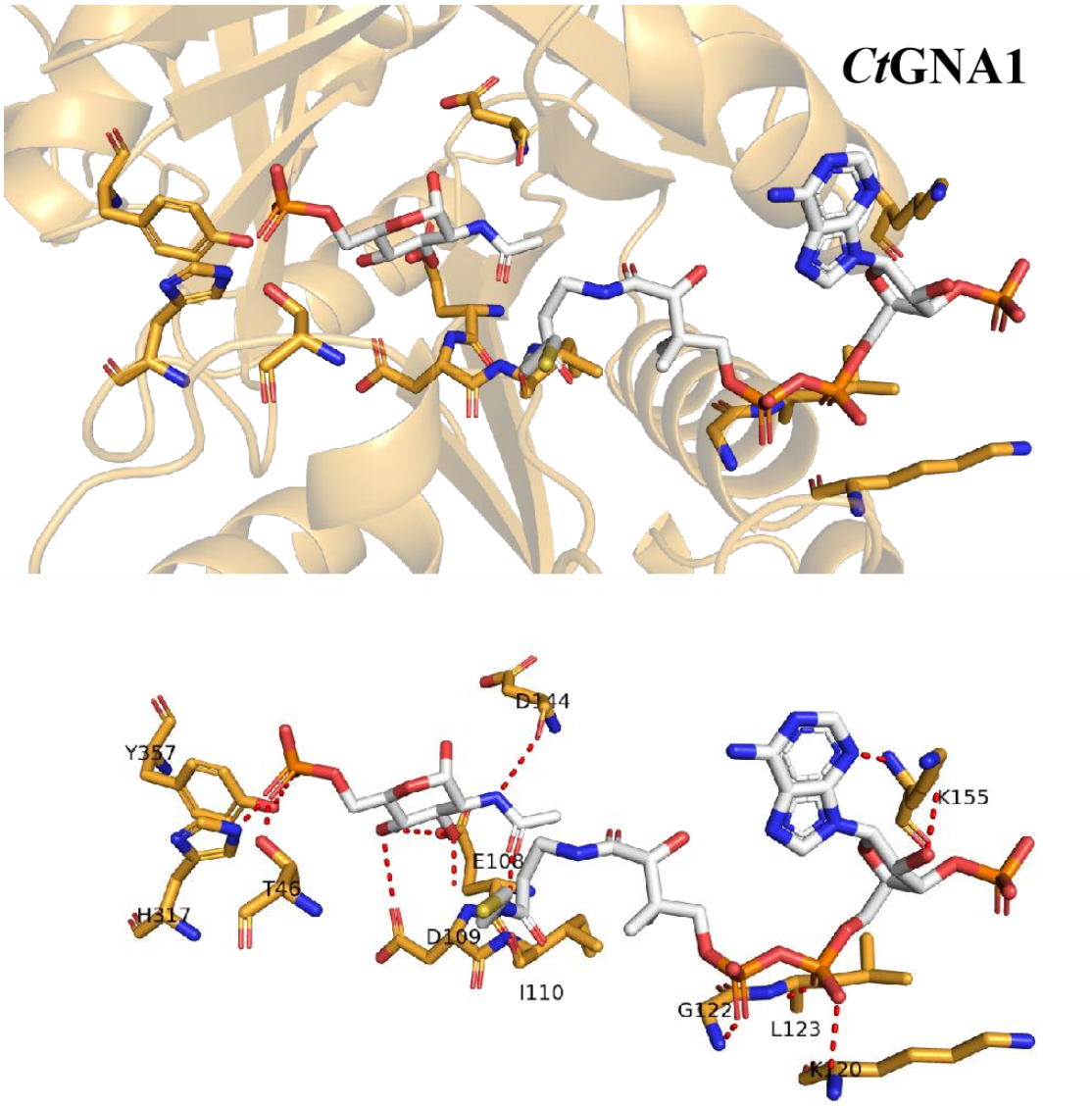

Figure S9. Calculated the number of hydrogen bonds bound to the products CoA and GlcNAc-6P for *Ct*GNA1, related to Figure 5.

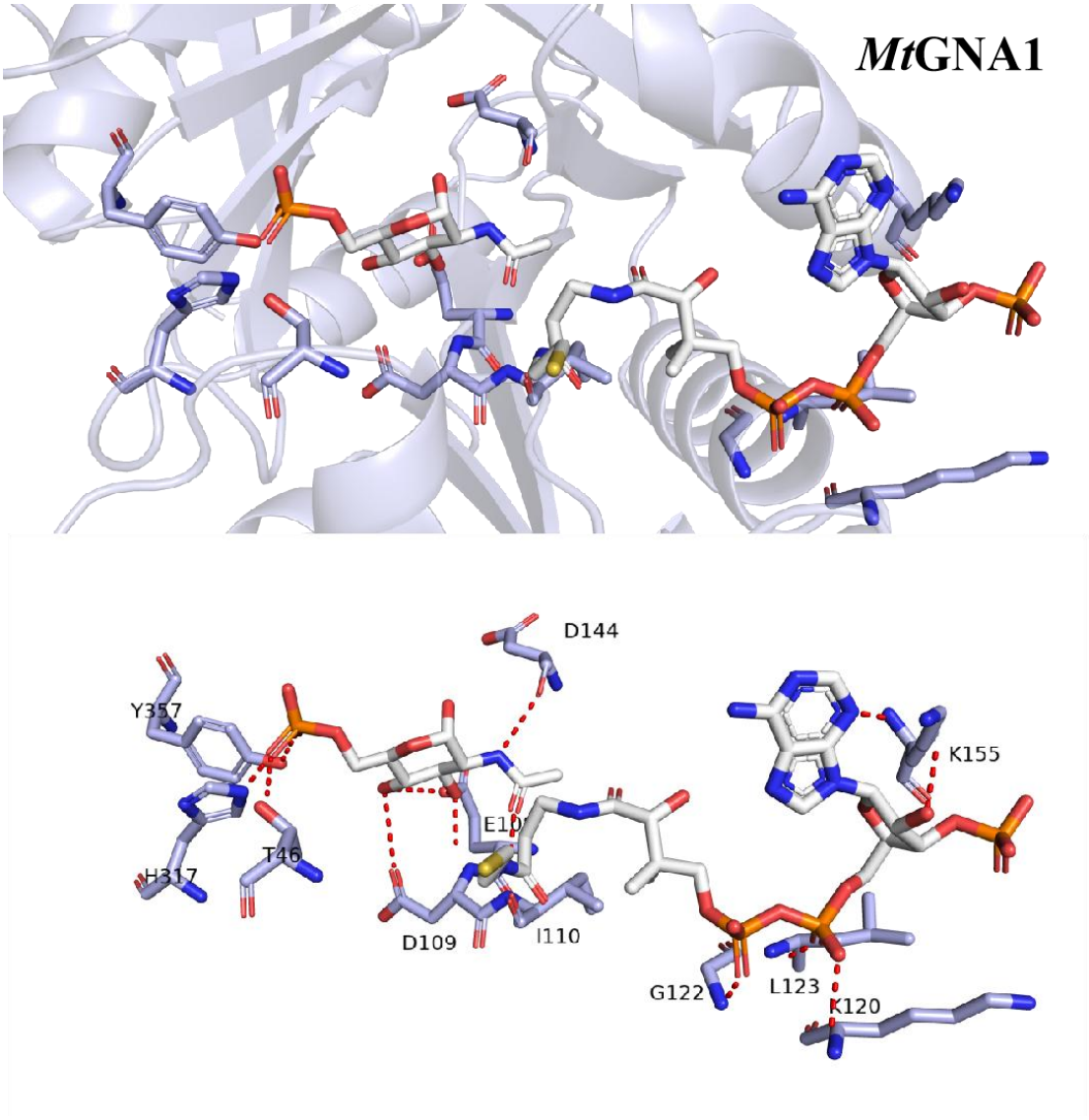

Figure S10. Calculated the number of hydrogen bonds bound to the products CoA and GlcNAc-6P for *Mt*GNA1, related to Figure 5.

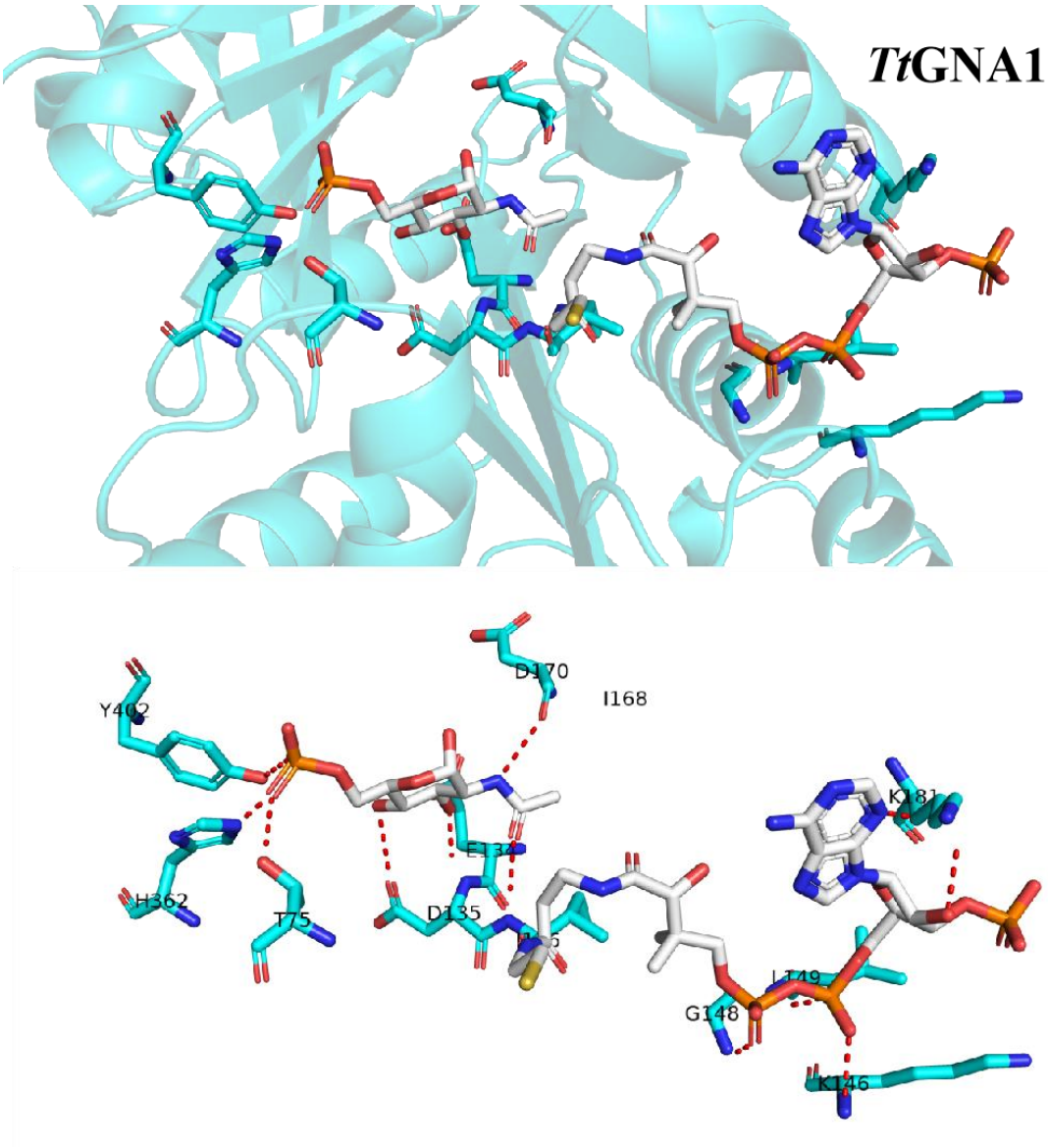

Figure S11. Calculated the number of hydrogen bonds bound to the products CoA and GlcNAc-6P for *Tt*GNA1, related to Figure 5.

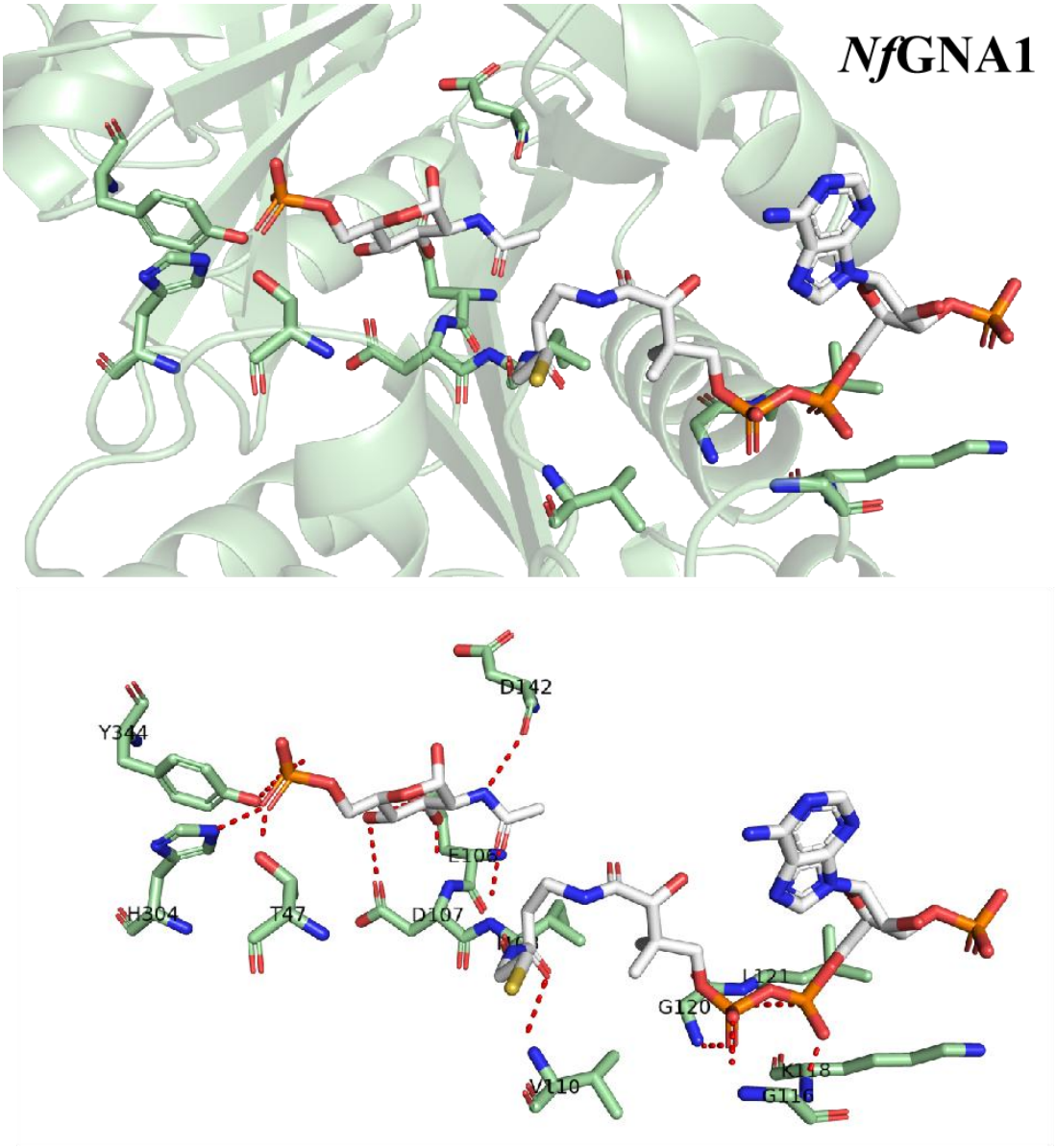

Figure S12. Calculated the number of hydrogen bonds bound to the products CoA and GlcNAc-6P for *Nf*GNA1, related to Figure 5.

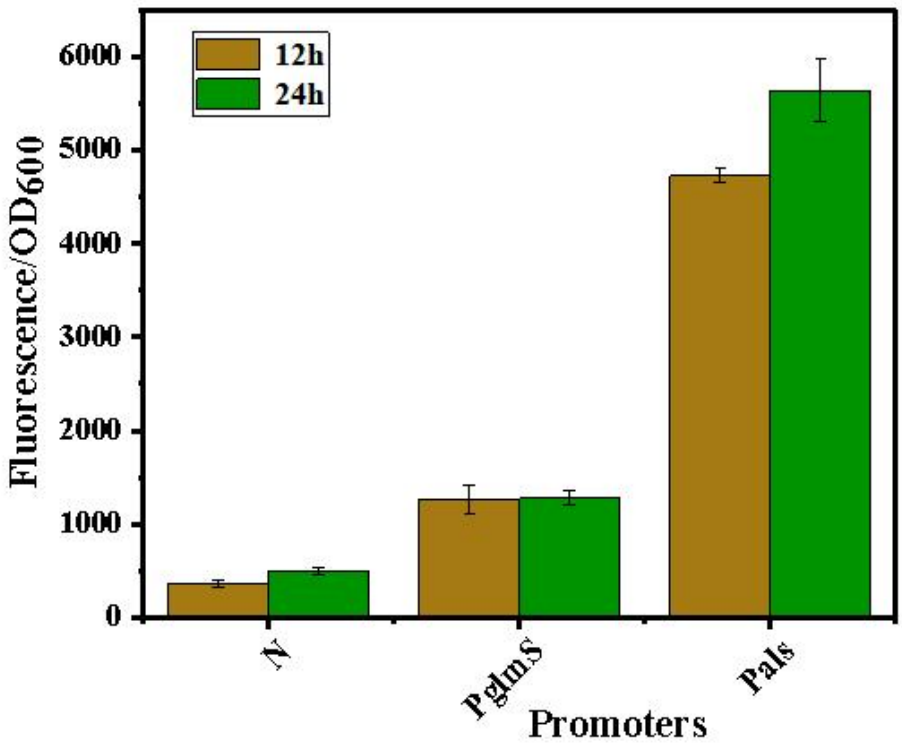

Figure S13. Characterization of P_{als} and P_{glmS} promoters in *B.licheniformis* MW3, related to Figure 5.

The strength of the promoters was characterized using *Sf*GFP as a reporter. N, negative control (promoter-less vector pHY300PLK). The fluorescence intensities were measured when the bacteria were cultured for 12h and 24h, respectively. The shake-flask fermentation medium was used for the experiment.

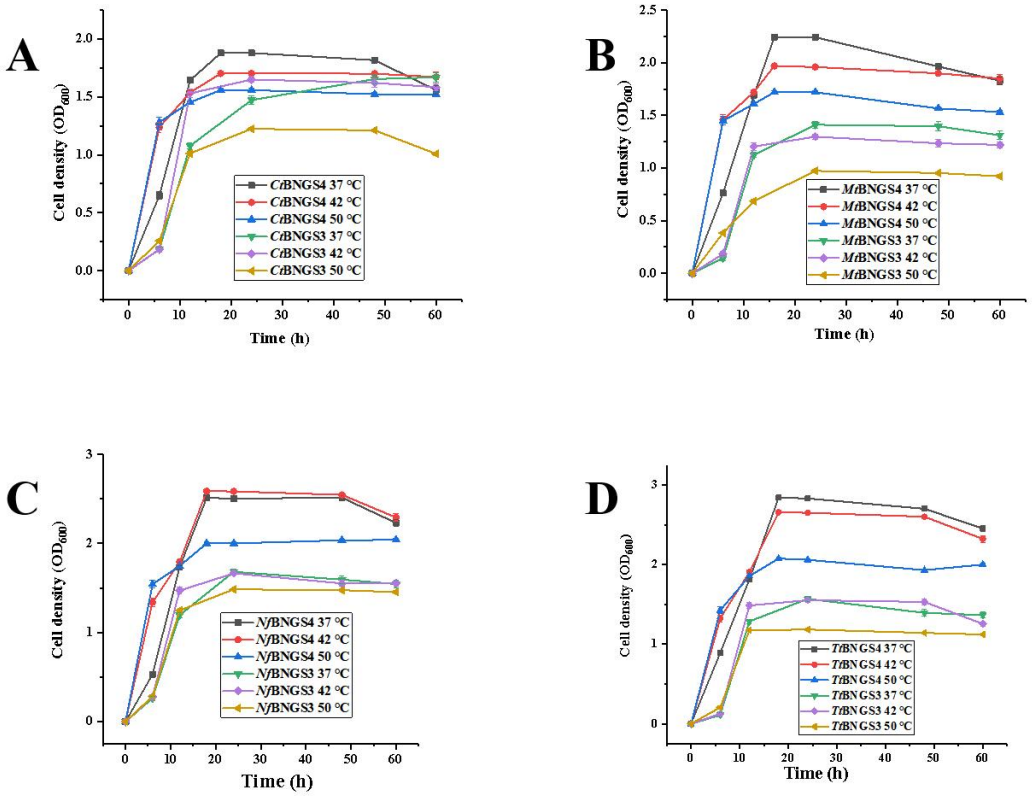

Figure S14. Bacterial growth curve determination in shake flasks, related to Figure 7.

(A) Growth curve of shake-flask fermentation for *Ct*BNGS3 and *Ct*BNGS4.

(B) Growth curve of shake-flask fermentation for *Mt*BNGS3 and *Mt*BNGS4.

(C) Growth curve of shake-flask fermentation for *Nf*BNGS3 and *Nf*BNGS4.

(D) Growth curve of shake-flask fermentation for *Tt*BNGS3 and *Tt*BNGS4.

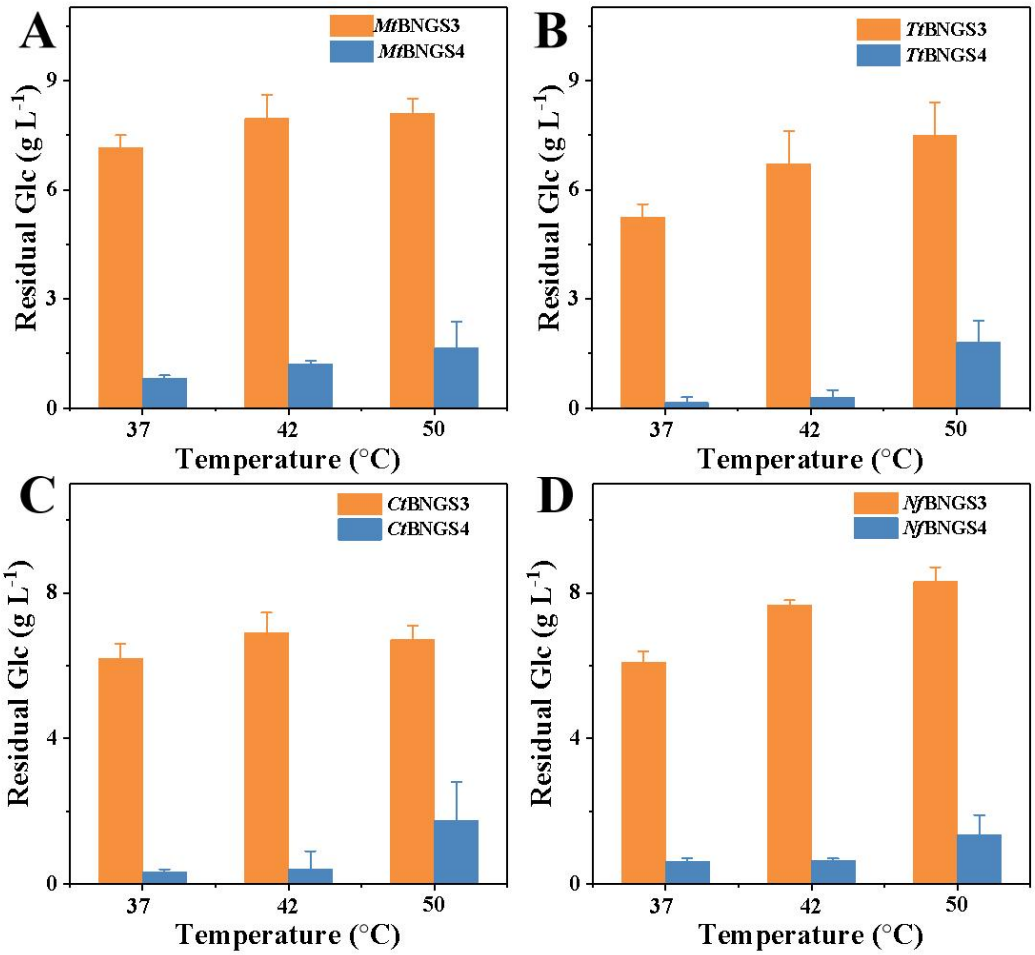

Figure S15. The residual glucose detection in shake flasks, related to Figure 7.

(A) The residual glucose of shake-flask fermentation for *Mt*BNGS3 and *Mt*BNGS4.

(B) The residual glucose of shake-flask fermentation for *Tt*BNGS3 and *Tt*BNGS4.

(C) The residual glucose of shake-flask fermentation for *Ct*BNGS3 and *Ct*BNGS4.

(D) The residual glucose of shake-flask fermentation for *Nf*BNGS3 and *Nf*BNGS4.

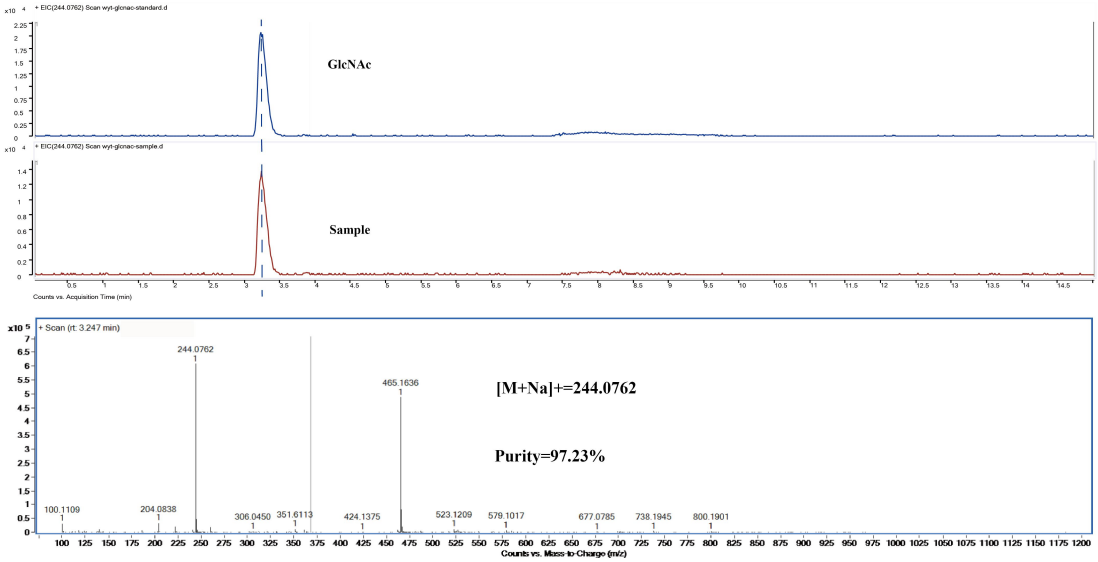

Figure S16. HPLC-MS detection of GlcNAc in purified sample for *Nf*BNGS4, related to Figure 7.

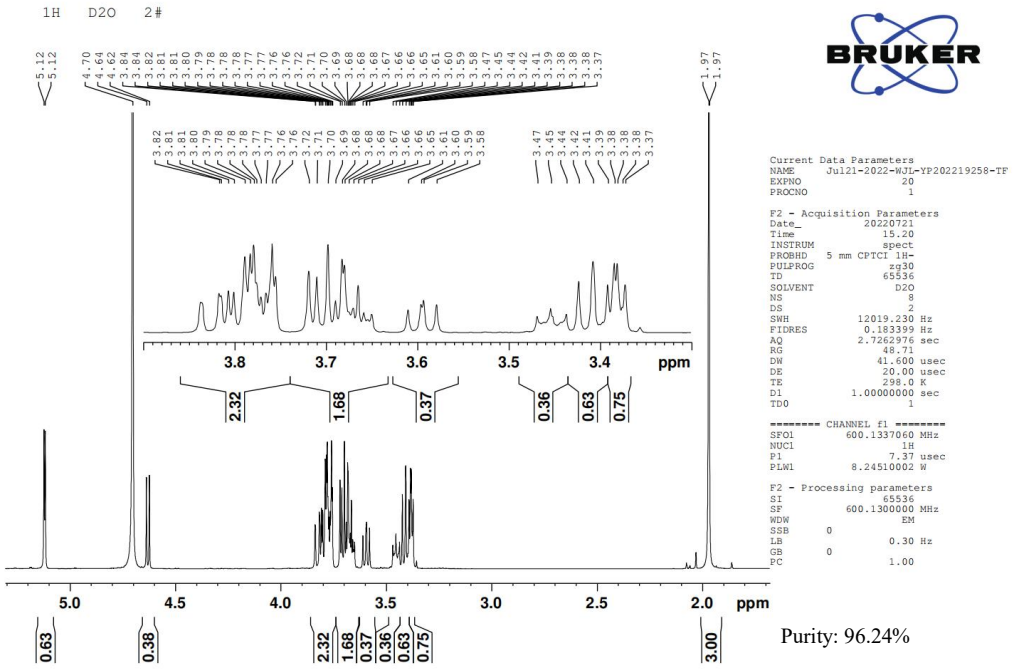

Figure S17. ^{1}HMR detection of GlcNAc in purified sample for *Nf*BNGS4, related to Figure 7.

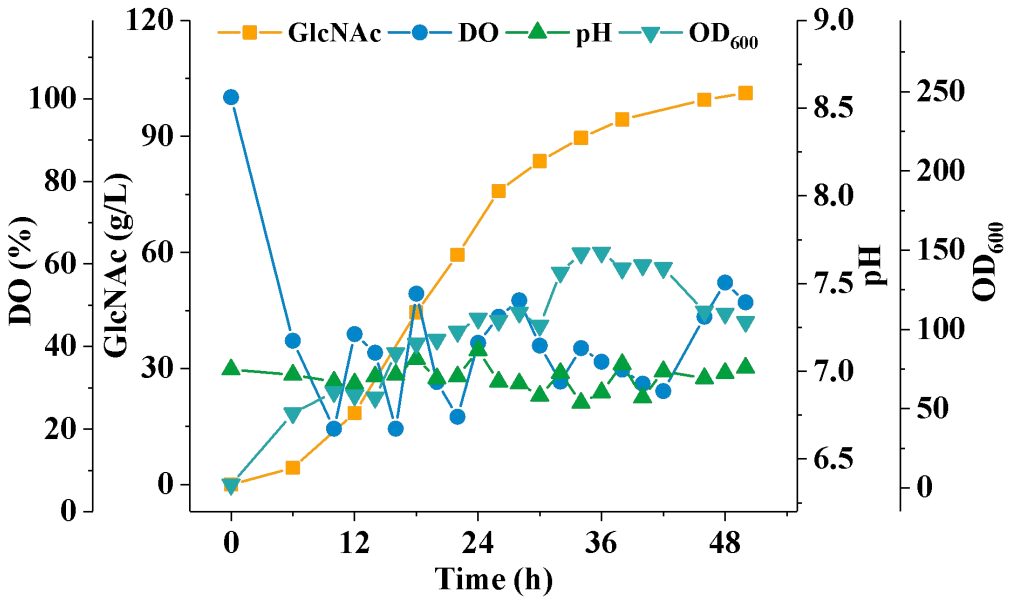

Figure S18. Production of GlcNAc in fed-batch fermentation in a 50-L bioreactor at 42℃ by *Tt*BNGS4, related to Figure 7.

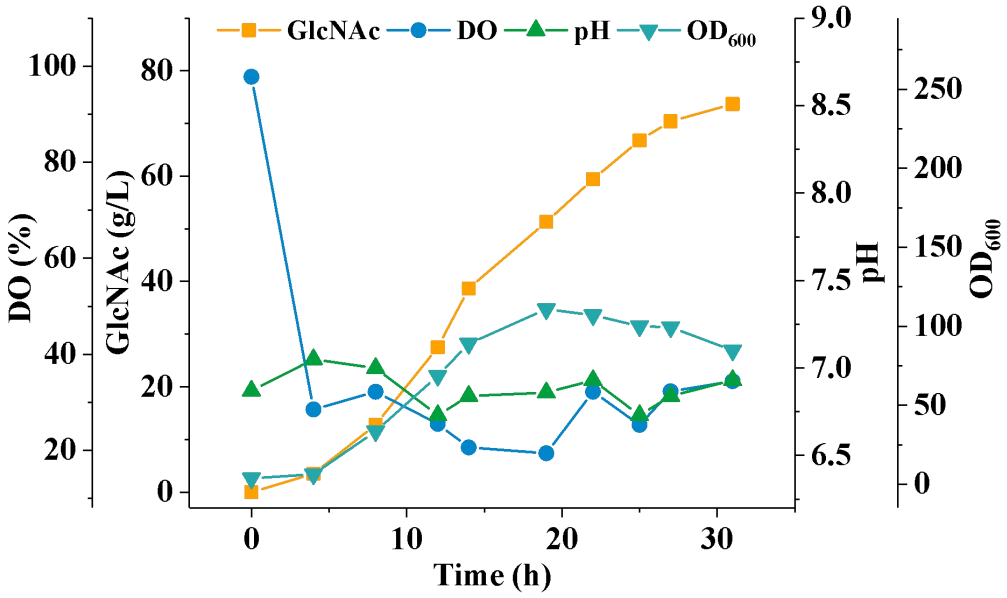

Figure S19. Production of GlcNAc in fed-batch fermentation in a 50-L bioreactor at 50℃ by *Tt*BNGS3, related to Figure 7.

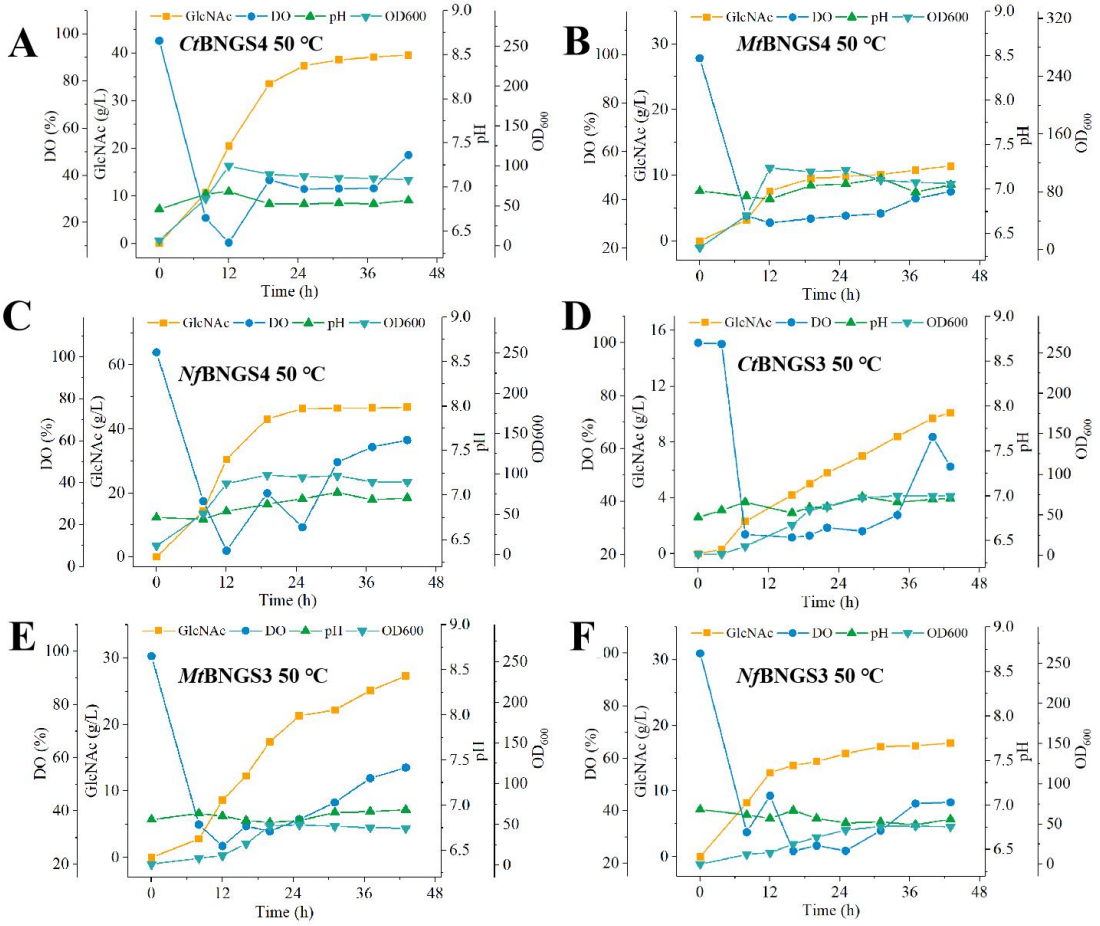

Figure S20. Production of GlcNAc in fed-batch fermentation in a 50-L bioreactor at 50 ℃, related to Figure 7.

(A) Fed-batch fermentation of *Ct*BNGS4 in a 50-L bioreactor at 50 ℃. OD_{600}, potical density at 600 nm.

(B) Fed-batch fermentation of *Mt*BNGS4 in a 50-L bioreactor at 50 ℃. OD_{600}, potical density at 600 nm.

(C) Fed-batch fermentation of *Nf*BNGS4 in a 50-L bioreactor at 50 ℃. OD_{600}, potical density at 600 nm.

(D) Fed-batch fermentation of *Ct*BNGS3 in a 50-L bioreactor at 50 ℃. OD_{600}, potical density at 600 nm.

(E) Fed-batch fermentation of *Mt*BNGS3 in a 50-L bioreactor at 50 ℃. OD_{600}, potical density at 600 nm.

(F) Fed-batch fermentation of *Nf*BNGS3 in a 50-L bioreactor at 50 ℃. OD_{600}, potical density at 600 nm.

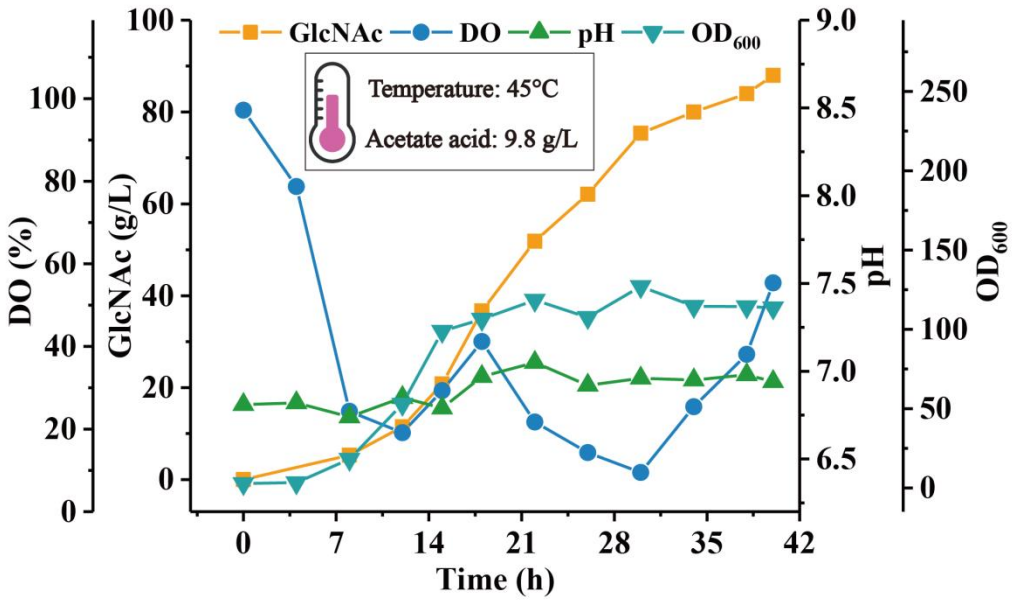

Figure S21. Production of GlcNAc in fed-batch fermentation in a 50-L bioreactor at 45℃ by *Tt*BNGS4, related to Figure 7.

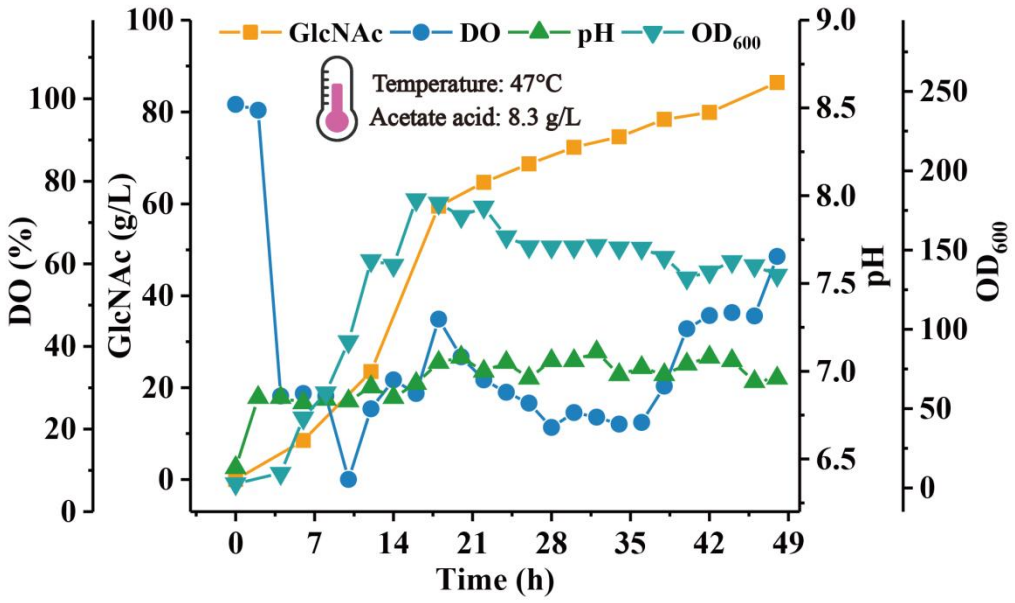

Figure S22. Production of GlcNAc in fed-batch fermentation in a 50-L bioreactor at 47℃ by *Tt*BNGS4, related to Figure 7.

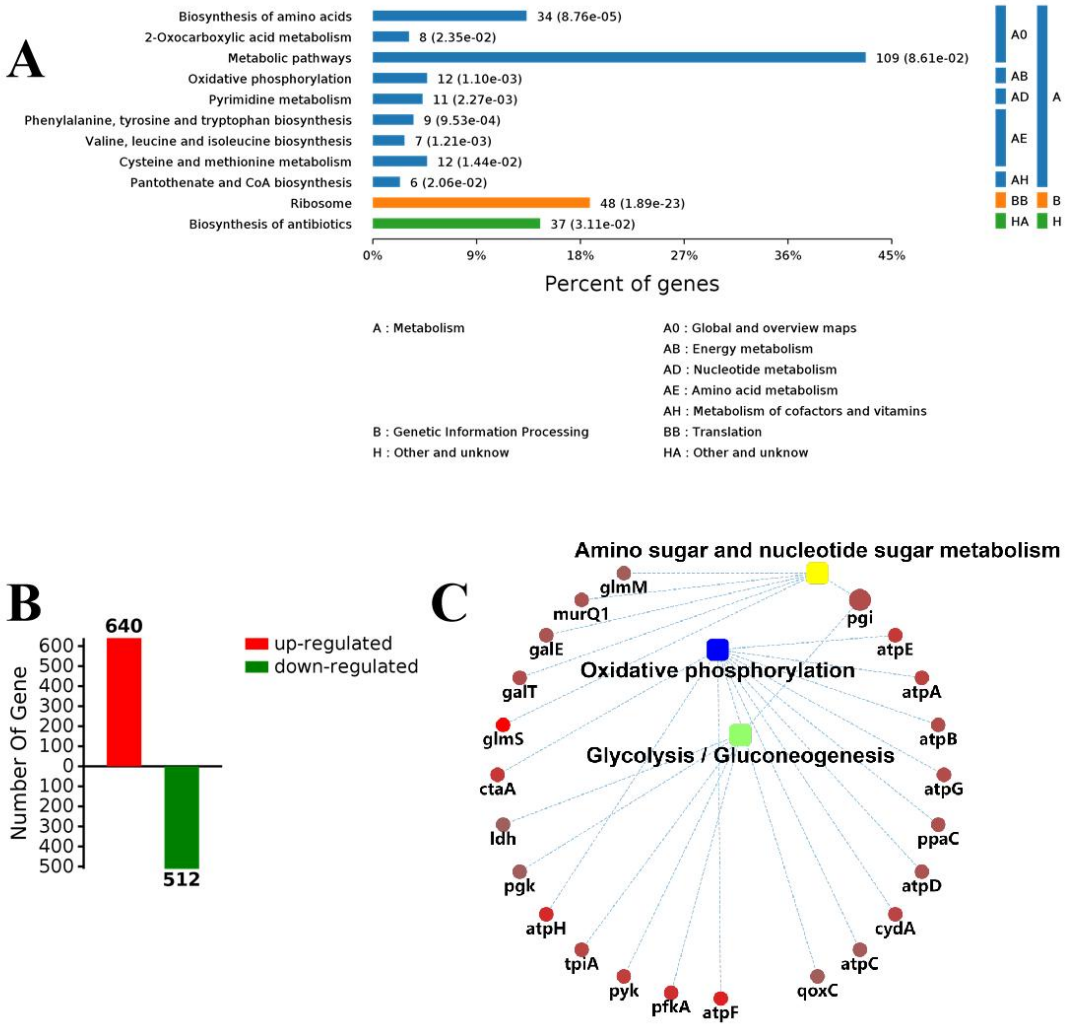

Figure S23. Transcriptome analysis comparison with BNGS4 and *Nf*BNGS4 in key metabolic pathway, related to Figure 8.

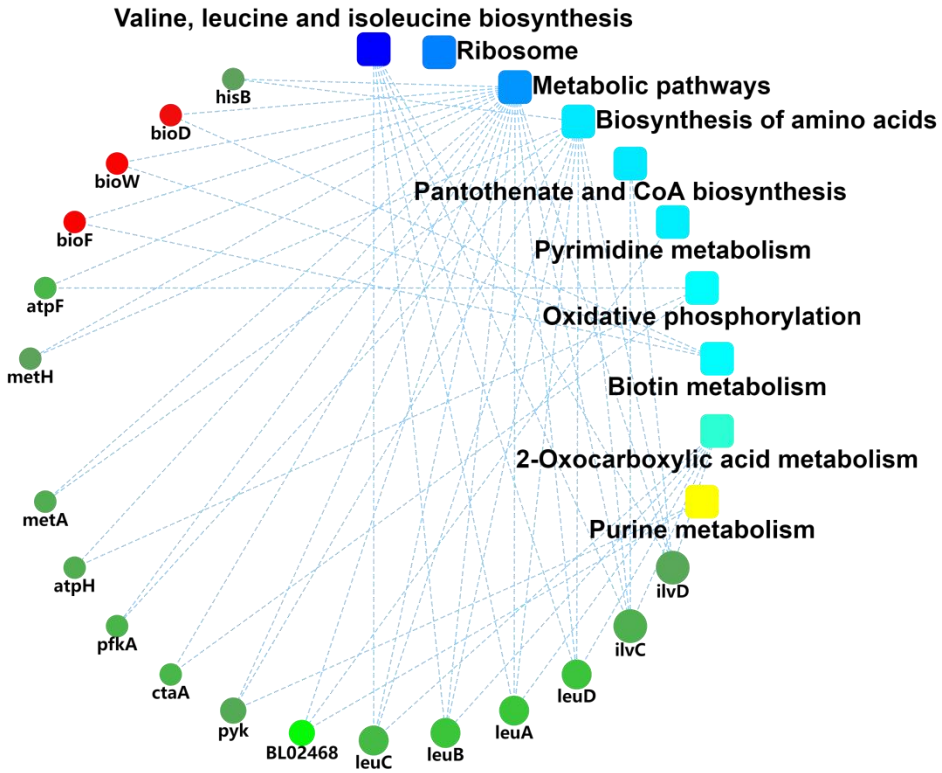

Figure S24. Transcriptome analysis comparison with *Tt*BNGS4 and *Nf*BNGS4 in key metabolic pathway, related to Figure 8.

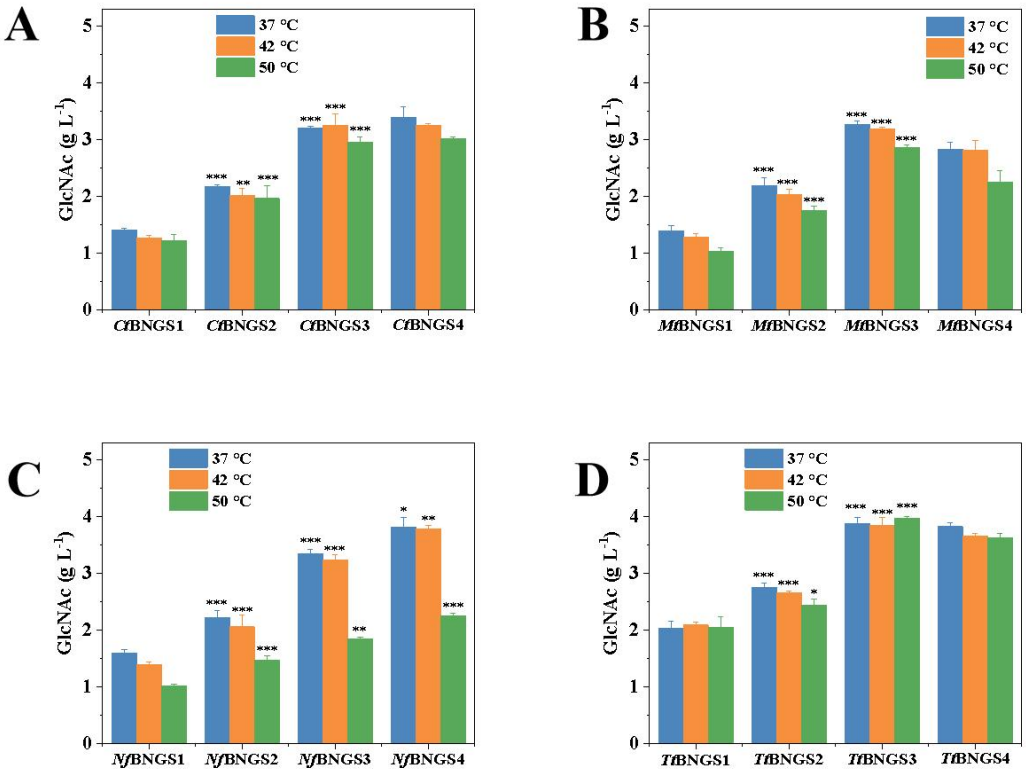

Figure S25. Shake-flask fermentation, related to Figure 7.

(A) Shake-flask fermentation of *Ct*BNGS1, *Ct*BNGS2, *Ct*BNGS3, and *Ct*BNGS4 at 37°C, 42°C, and 50°C, respectively. Triplicate experiments were carried out for physiological measurements, and error bars represent standard deviation. *p<0.05, **p<0.01, ***p<0.001 as determined by t test.

(B) Shake-flask fermentation of *Mt*BNGS1, *Mt*BNGS2, *Mt*BNGS3, and *Mt*BNGS4 at 37°C, 42°C, and 50°C, respectively. Triplicate experiments were carried out for physiological measurements, and error bars represent standard deviation. *p<0.05, **p<0.01, ***p<0.001 as determined by t test.

(C) Shake-flask fermentation of *Nf*BNGS1, *Nf*BNGS2, *Nf*BNGS3, and *Nf*BNGS4 at 37°C, 42°C, and 50°C, respectively. Triplicate experiments were carried out for physiological measurements, and error bars represent standard deviation. *p<0.05, **p<0.01, ***p<0.001 as determined by t test.

(D) Shake-flask fermentation of *Tt*BNGS1, *Tt*BNGS2, *Tt*BNGS3, and *Tt*BNGS4 at 37°C, 42°C, and 50°C, respectively. Triplicate experiments were carried out for physiological measurements, and error bars represent standard deviation. *p<0.05, **p<0.01, ***p<0.001 as determined by t test.

Supplementary Tables

Table S1 Screened GNA1 candidate thermophilic enzymes based on thermophilic fungi database, related to Figure 2.

Number	Genome Acc. No.	Score	E-Value	Protein ID and Annotation
1	Talth1p4.representatives	308	2.16E-35	Talth1p4_004467
2	Dacth1p7.accepted	305	1.07E-34	Dacth1p7_004956
3	Calth2p4.representatives	303	1.26E-34	Calth2p4_002930
4	Thela2p4.representatives	302	1.73E-34	Thela2p4_001470
5	Paeby1p7.accepted	298	5.80E-34	Paeby1p7_013401
6	Theau2p4.representatives	296	2.33E-33	Theau2p4_007854
7	Talth1p4.representatives	289	3.68E-32	Talth1p4_001395
8	Thela2p4.representatives	287	6.43E-32	Thela2p4_003400
9	Rhipu1p4.representatives	284	8.01E-32	Rhipu1p4_009376
10	Paeby1p7.accepted	288	8.23E-32	Paeby1p7_002255
11	Acrth2p7.accepted	283	9.43E-32	Acrth2p7_012607
12	Thest2p7.accepted	282	1.53E-31	Thest2p7_018758
13	Corth2p4.representatives	282	1.67E-31	Corth2p4_004224
14	Myrth2p4.representatives	278	5.62E-31	Myrth2p4_006746
15	Spoth2p4.representatives	278	6.06E-31	Spoth2p4_009953
16	Scyth2p4.representatives	277	8.16E-31	Scyth2p4_002266
17	Chath2p7.accepted	277	1.08E-30	Chath2p7_007107
18	Thite2p4.representatives	275	1.90E-30	Thite2p4_002933
19	Thiau2p7.accepted	274	2.40E-30	Thiau2p7_011322
20	Humhy2p7.accepted	263	1.18E-28	Humhy2p7_018757
21	Calth2p4.representatives	242	1.45E-25	Calth2p4_007804
22	Acrth2p7.accepted	239	5.00E-25	Acrth2p7_011569
23	CBS620.91p7.accepted	234	5.06E-25	CBS620.91p7_001600
24	Rhipu1p4.representatives	210	1.05E-20	Rhipu1p4_001988
25	Calth2p4.representatives	96	0.000257906	Calth2p4_004126
26	Humhy2p7.accepted	95	0.000458471	Humhy2p7_011674
27	Rhipu1p4.representatives	91	0.00128448	Rhipu1p4_002247
28	Chath2p7.accepted	88	0.00321645	Chath2p7_017277
29	Corth2p4.representatives	86	0.00374988	Corth2p4_002251
30	CBS620.91p7.accepted	85	0.00878263	CBS620.91p7_000313
31	Myrth2p4.representatives	83	0.00968691	Myrth2p4_005675

Note: Number 1, 2, 8, 10, 11, 14, 16, and 17 have been screened.

Table S2 Tm index and aliphatic index of GNA1 candidate thermophilic enzymes based on Uniprot database, related to Figure 2.

Number	GNA1 enzyme from	Tm Index	Aliphatic Index
1	*Kluyveromyces lactis*	2.3148	112.3404
2	*Phycomyces blakesleeanus*	1.9162	111.6667
3	*Aphanomyces astaci*	2.4129	108.2877
4	*Kuraishia capsulata*	1.8453	107.0395
5	*Cryptococcus gattii* CA1280	1.8672	107.0186
6	*Panicum hallii*	1.7310	106.8987
7	*Anaeromyces robustus*	1.8783	105.7143
8	*Hymenolepis nana*	2.0458	103.4737
9	*Nadsonia fulvescens*	2.7142	103.3533
10	*Aureobasidium pullulans*	1.9133	102.7517
11	*Magnaporthiopsis poae*	2.0930	102.1637
12	*Oncopeltus fasciatus*	2.4285	101.8782
13	*Echinococcus multilocularis*	2.1024	101.7978
14	*Lachancea meyersii*	2.0759	100.3822
15	*Saccharomyces cerevisiae*	1.6119	94.3396

Note: Number 1, 2, 3, 5, 6, 8, 9, and 11 have been screened.

The TI (Tm Index) method is provided as a free software platform composed of a dipeptide Tm (melting temperature) weight value table and a web-based interface (Online Tm Predictor, see also http://tm.life.nthu.edu.tw/). The higher the TI value, the more stable the enzyme is.

The aliphatic index shows the thermal stability of the enzyme sequences and larger index confirmed the enzyme for higher stability.

Table S3 Enzyme kinetic parameters of *Tt*GNA1, *Mt*GNA1, *Nf*GNA1, and *Ct*GNA1, related to Figure 4 and STAR Methods.

Enzyme	GlcN-6P K_m (mM)	Ac-CoA K_m (mM)	GlcN-6P k_{cat} (s^{-1})	Ac-CoA k_{cat} (s^{-1})	GlcN-6P k_{cat}/K_m (s^{-1} mM^{-1})	Ac-CoA k_{cat}/K_m (s^{-1} mM^{-1})
*Tt*GNA1	0.45	0.49	840.40	792.53	1867.56	1671.41
*Nf*GNA1	1.67	2.11	538.61	504.27	322.52	238.99
*Ct*GNA1	0.26	0.36	472.53	568.90	1817.43	1580.29
*Mt*GNA1	0.35	0.83	617.71	633.94	1764.88	763.78
*Sc*GNA1	1.08	1.76	181.39	279.59	167.95	158.86

Table S4 Putative stabilizing factors of *Tt*GNA1, *Mt*GNA1, *Nf*GNA1, *Sc*GNA1, and *Ct*GNA1, related to Figure 5 and STAR Methods.

Enzyme	Numbe of helice	β-branched residue content in helices (%)	β-branched residue content in the whole sequence (%)
*Tt*GNA1	8	15.3	17.75
*Nf*GNA1	7	19.3	22.16
*Mt*GNA1	7	11.8	21.35
*Ct*GNA1	7	14.7	16.85
*Sc*GNA1	6	17.9	23.90

Table S5 Flexibility indices of *Tt*GNA1, *Mt*GNA1, *Nf*GNA1, and *Ct*GNA1, related to Figure 5 and STAR Methods.

Enzyme	F
*Tt*GNA1	0.9703
*Nf*GNA1	0.9839
*Mt*GNA1	0.9866
*Ct*GNA1	0.9862

Table S6 The previous reported strains for GlcNAc production with glucose as the sole carbon source, related to Discussion.

Strains	Fermentation temperature (°C)	GlcNAc titers (g/L)	Reference
Escherichia coli 7107-607	37	110	[1]
Saccharomyces cerevisiae 2627MY	30	3.114	[2]
Bacillus subtilis FMIP34	37	87.5	[3]
Corynebacterium glutamicum CGGN4mdhM7-GNA1-CgglmS-RamAMA	30	117.1 ± 1.9	[4]
Bacillus licheniformis *Nf*BNGS4	42	119.3	This study
Bacillus licheniformis *Tt*BNGS4	47	86.4	This study
Bacillus licheniformis *Tt*BNGS4	From 42 to 50 with temperature programming	83	This study

Table S7 Strains used in this study, related to STAR Methods.

Name	Characteristics	Source
B. licheniformis MW3	Mutant strains of *B. licheniformis* ATCC14580 (Δ*hsdR1*, Δ*hsdR2*)	Laboratory stock
BNGS1	*B. licheniformis* MW3 derivate, MW3Δ*nagP1*Δ*nagP2*Δ*gamA*Δ*nagA*Δ*nagB*	This work
*Sc*BNGS1	BNGS1 derivate, harboring pHY300PLK-P_{als}-*Scgna1*	This work
*Scop*BNGS1	BNGS1 derivate, harboring pHY300PLK-P_{als}-*Scopgna1*	This work
BNGS1-P_{43}-*ScopGNA1*	BNGS1 derivate, harboring pHY300PLK-P_{43}-*Scopgna1*	This work
BNGS1-P_{aprE}-*ScopGNA1*	BNGS1 derivate, harboring pHY300PLK-P_{aprE}-*Scopgna1*	This work
BNGS1-P_{st}-*ScopGNA1*	BNGS1 derivate, harboring pHY300PLK-P_{st}-*Scopgna1*	This work
BNGS1-P_{bl9}-*ScopGNA1*	BNGS1 derivate, harboring pHY300PLK-P_{bl9}-*Scopgna1*	This work
*Tt*BNGS1	BNGS1 derivate, harboring pHY300PLK-P_{als}-*Ttgna1*	This work
*Mt*BNGS1	BNGS1 derivate, harboring pHY300PLK-P_{als}-*Mtgna1*	This work
*Ct*BNGS1	BNGS1 derivate, harboring pHY300PLK-P_{als}-*Ctgna1*	This work
*Nf*BNGS1	BNGS1 derivate, harboring pHY300PLK-P_{als}-*Nfgna1*	This work
*Kl*BNGS1	BNGS1 derivate, harboring pHY300PLK-P_{als}-*Klgna1*	This work
*Pb*BNGS1	BNGS1 derivate, harboring pHY300PLK-P_{als}-*Pbgna1*	This work
*Aa*BNGS1	BNGS1 derivate, harboring pHY300PLK-P_{als}-*Aagna1*	This work
*Cg*BNGS1	BNGS1 derivate, harboring pHY300PLK-P_{als}-*Cggna1*	This work
*Ph*BNGS1	BNGS1 derivate, harboring pHY300PLK-P_{als}-*Phgna1*	This work
*Hn*BNGS1	BNGS1 derivate, harboring pHY300PLK-P_{als}-*Hngna1*	This work
*Mp*BNGS1	BNGS1 derivate, harboring pHY300PLK-P_{als}-*Mpgna1*	This work
*Lf*BNGS1	BNGS1 derivate, harboring pHY300PLK-P_{als}-*Lfgna1*	This work
*Rf*BNGS1	BNGS1 derivate, harboring	This work

	pHY300PLK-P_{als}-*Rfgna1*	
*Cf*BNGS1	BNGS1 derivate, harboring pHY300PLK-P_{als}-*Cfgna1*	This work
*Fn*BNGS1	BNGS1 derivate, harboring pHY300PLK-P_{als}-*Fngna1*	This work
*Td*BNGS1	BNGS1 derivate, harboring pHY300PLK-P_{als}-*Tdgna1*	This work
*Tl*BNGS1	BNGS1 derivate, harboring pHY300PLK-P_{als}-*Tlgna1*	This work
*Rb*BNGS1	BNGS1 derivate, harboring pHY300PLK-P_{als}-*Rbgna1*	This work
*At*BNGS1	BNGS1 derivate, harboring pHY300PLK-P_{als}-*Atgna1*	This work
*Mf*BNGS1	BNGS1 derivate, harboring pHY300PLK-P_{als}-*Mfgna1*	This work
BNGS2	*B. licheniformis* MW3 derivate, MW3Δ*nagP1*Δ*nagP2*Δ*gamA*Δ*nagA*Δ*nagB*::P_{als}-*BlglmS*	This work
*Scop*BNGS2	BNGS2 derivate, harboring pHY300PLK-P_{als}-*Scopgna1*	This work
*Tt*BNGS2	BNGS2 derivate, harboring pHY300PLK-P_{als}-*Ttgna1*	This work
*Mt*BNGS2	BNGS2 derivate, harboring pHY300PLK-P_{als}-*Mtgna1*	This work
*Ct*BNGS2	BNGS2 derivate, harboring pHY300PLK-P_{als}-*Ctgna1*	This work
*Nf*BNGS2	BNGS2 derivate, harboring pHY300PLK-P_{als}-*Nfgna1*	This work
BNGS3	*B.licheniformis* MW3 derivate, MW3Δ*nagP1*Δ*nagP2*Δ*gamA*Δ*nagA*Δ*nagB*Δ*alsS*Δ*alsD*::P_{als}-*BlglmS*	This work
*Scop*BNGS3	BNGS1 derivate, harboring pHY300PLK-P_{als}-*Scopgna1*	This work
*Tt*BNGS3	BNGS3 derivate, harboring pHY300PLK-P_{als}-*Ttgna1*	This work
*Mt*BNGS3	BNGS3 derivate, harboring pHY300PLK-P_{als}-*Mtgna1*	This work
*Ct*BNGS3	BNGS3 derivate, harboring pHY300PLK-P_{als}-*Ctgna1*	This work
*Nf*BNGS3	BNGS3 derivate, harboring pHY300PLK-P_{als}-*Nfgna1*	This work
*Tt*BNGS4	BNGS3 derivate, MW3Δ*nagP1*Δ*nagP2*Δ*gamA*Δ*nagA*Δ*nagB*Δ*alsS*Δ*alsD*::P_{als}-*BlglmS*::P_{als}-*Ttgna1*	This work

*Mt*BNGS4	BNGS3 derivate, MW3Δ*nagP1*Δ*nagP2*Δ*gamA*Δ*nagA*Δ*nagB*Δ*als SΔalsD*::P_{als}-*BlgImS*::P_{als}-*Mtgna1*	This work
*Ct*BNGS4	BNGS3 derivate, MW3Δ*nagP1*Δ*nagP2*Δ*gamA*Δ*nagA*Δ*nagB*Δ*als SΔalsD*::P_{als}-*BlgImS*::P_{als}-*Ctgna1*	This work
*Nf*BNGS4	BNGS3 derivate, MW3Δ*nagP1*Δ*nagP2*Δ*gamA*Δ*nagA*Δ*nagB*Δ*als SΔalsD*::P_{als}-*BlgImS*::P_{als}-*Nfgna1*	This work
E. coli BL21 (DE3)	Host for gene expression and cloning the *gna1* gene	Laboratory stock
E. coli S17-1	Conjugative strain able to host λ-*pir*-dependent plasmids	Laboratory stock
E. coli BL21(pETDuet-*Mtgna1*)	*E. coli* BL21(DE3) harboring pETDuet-*Mtgna1*	This study
E. coli BL21(pETDuet-*Nfgna1*)	*E. coli* BL21(DE3) harboring pETDuet-*Nfgna1*	This study
E. coli BL21(pETDuet-*Ctgna1*)	*E. coli* BL21(DE3) harboring pETDuet-*Ctgna1*	This study
E. coli BL21(pETDuet-*Ttgna1*)	*E. coli* BL21(DE3) harboring pETDuet-*Ttgna1*	This study
E. coli BL21(pETDuet-*Scopgna1*)	*E. coli* BL21(DE3) harboring pETDuet-*Scopgna1*	This study

Table S8 Plasmids used in this study, related to STAR Methods.

Name	Characteristics	Source
pHY300PLK	*E.coli-B.licheniformis* shuttle vector, *Amp*^{r},*Tet*^{r}	Laboratory stock
pKVM1	Gene knockout and insertion vector, *Ery*^{r}, *Amp*^{r}	Laboratory stock
pETDuet-1	*PT7*, overexpression vector, *Amp*^{r}	Laboratory stock
pETDuet-*Mtgna1*	pETDuet-1 contained the *Mtgna1* gene, *Amp*^{r}	This study
pETDuet-*Nfgna1*	pETDuet-1 contained the *Nfgna1* gene, *Amp*^{r}	This study
pETDuet-*Ctgna1*	pETDuet-1 contained the *Ctgna1* gene, *Amp*^{r}	This study
pETDuet-*Ttgna1*	pETDuet-1 contained the *Ttgna1* gene, *Amp*^{r}	This study
pETDuet-*Scopgna1*	pETDuet-1 contained the *Scopgna1* gene, *Amp*^{r}	This study
pHY300PLK-P$_{als}$-*Scopgna1*	pHY300PLK contained P$_{als}$-*Scopgna1*, *Amp*^{r},*Tet*^{r}	This study
pHY300PLK-P$_{43}$-*Scopgna1*	pHY300PLK contained P$_{43}$-*Scopgna1*, *Amp*^{r},*Tet*^{r}	This study
pHY300PLK-P$_{aprE}$-*Scopgna1*	pHY300PLK contained P$_{aprE}$-*Scopgna1*, *Amp*^{r},*Tet*^{r}	This study
pHY300PLK-P$_{st}$-*Scopgna1*	pHY300PLK contained P$_{st}$-*Scopgna1*, *Amp*^{r},*Tet*^{r}	This study
pHY300PLK-P$_{bl9}$-*Scopgna1*	pHY300PLK contained P$_{bl9}$-*Scopgna1*, *Amp*^{r},*Tet*^{r}	This study
pHY300PLK-P$_{als}$-*Scgna1*	pHY300PLK contained P$_{als}$-*Scgna1*, *Amp*^{r},*Tet*^{r}	This study
pHY300PLK-P$_{als}$-*Ttgna1*	pHY300PLK contained P$_{als}$-*Ttgna1*, *Amp*^{r},*Tet*^{r}	This study
pHY300PLK-P$_{als}$-*Ctgna1*	pHY300PLK contained P$_{als}$-*Ctgna1*, *Amp*^{r},*Tet*^{r}	This study
pHY300PLK-P$_{als}$-*Mtgna1*	pHY300PLK contained P$_{als}$-*Mtgna1*, *Amp*^{r},*Tet*^{r}	This study
pHY300PLK-P$_{als}$-*Nfgna1*	pHY300PLK contained P$_{als}$-*Nfgna1*, *Amp*^{r},*Tet*^{r}	This study
pHY300PLK-P$_{als}$-*Klgna1*	pHY300PLK contained P$_{als}$-*Klgna1*, *Amp*^{r},*Tet*^{r}	This study
pHY300PLK-P$_{als}$-*Pbgna1*	pHY300PLK contained P$_{als}$-*Pbgna1*, *Amp*^{r},*Tet*^{r}	This study
pHY300PLK-P$_{als}$-*Aagna1*	pHY300PLK contained P$_{als}$-*Aagna1*, *Amp*^{r},*Tet*^{r}	This study
pHY300PLK-P$_{als}$-*Cggna1*	pHY300PLK contained P$_{als}$-*Cggna1*, *Amp*^{r},*Tet*^{r}	This study
pHY300PLK-P$_{als}$-*Phgna1*	pHY300PLK contained P$_{als}$-*Phgna1*, *Amp*^{r},*Tet*^{r}	This study
pHY300PLK-P$_{als}$-*Hngna1*	pHY300PLK contained P$_{als}$-*Hngna1*, *Amp*^{r},*Tet*^{r}	This study
pHY300PLK-P$_{als}$-*Mpgna1*	pHY300PLK contained P$_{als}$-*Mpgna1*, *Amp*^{r},*Tet*^{r}	This study
pHY300PLK-P$_{als}$-*Lfgna1*	pHY300PLK contained P$_{als}$-*Lfgna1*, *Amp*^{r},*Tet*^{r}	This study
pHY300PLK-P$_{als}$-*Rfgna1*	pHY300PLK contained P$_{als}$-*Rfgna1*, *Amp*^{r},*Tet*^{r}	This study
pHY300PLK-P$_{als}$-*Cfgna1*	pHY300PLK contained P$_{als}$-*Cfgna1*, *Amp*^{r},*Tet*^{r}	This study
pHY300PLK-P$_{als}$-*Fngna1*	pHY300PLK contained P$_{als}$-*Fngna1*, *Amp*^{r},*Tet*^{r}	This study
pHY300PLK-P$_{als}$-*Tdgna1*	pHY300PLK contained P$_{als}$-*Tdgna1*, *Amp*^{r},*Tet*^{r}	This study
pHY300PLK-P$_{als}$-*Tlgna1*	pHY300PLK contained P$_{als}$-*Tlgna1*, *Amp*^{r},*Tet*^{r}	This study

pHY300PLK-P$_{als}$-*Rbgna1*	pHY300PLK contained P$_{als}$-*Rbgna1*, *Amp^r*,*Tet^r*	This study
pHY300PLK-P$_{als}$-*Atgna1*	pHY300PLK contained P$_{als}$-*Atgna1*, *Amp^r*,*Tet^r*	This study
pHY300PLK-P$_{als}$-*Mfgna1*	pHY300PLK contained P$_{als}$-*Mfgna1*, *Amp^r*,*Tet^r*	This study
pHY300PLK-P$_{als}$-*Klgna1*	pHY300PLK contained P$_{als}$-*Klgna1*, *Amp^r*,*Tet^r*	This study
pHY300PLK-P$_{als}$-*Pbgna1*	pHY300PLK contained P$_{als}$-*Pbgna1*, *Amp^r*,*Tet^r*	This study
pHY300PLK-P$_{als}$-*Aagna1*	pHY300PLK contained P$_{als}$-*Aagna1*, *Amp^r*,*Tet^r*	This study
pKVMΔ*nagP1*	Vector for deletion of *nagP1* gene in *B. licheniformis* MW3, *Ery^r, Amp^r*	This study
pKVMΔ*nagP2*	Vector for deletion of *nagP2* gene in *B. licheniformis* MW3, *Ery^r, Amp^r*	This study
pKVMΔ*nagAB*	Vector for deletion of *nagA* and *nagB* genes in *B. licheniformis* MW3, *Ery^r, Amp^r*	This study
pKVMΔ*gamA*	Vector for deletion of *gamA* gene in *B. licheniformis* MW3, *Ery^r, Amp^r*	This study
pKVM-P*als-glmS*	Vector for overexpression of *glmS* gene in *B. licheniformis* MW3, *Ery^r, Amp^r*	This study
pKVMΔ*alsSD*	Vector for deletion of *alsS* and *alsD* gene in *B. licheniformis* MW3, *Ery^r, Amp^r*	This study

Abbreviations: *Ery^r*, erythromycin resistance; *Amp^r*, ampicillin resistance; *Tet^r*, tetracycline resistance.

Table S9 Primers used in this study, related to STAR Methods.

Primer	Sequence 5'-3'
nagP-U-F	GGTACCCGGGAGCTCATGAATGAGGAGGATCACACAGTC
nagP-U-R	GAAGGGGCTTATCTTAGTTAAAACCCCTTTCGATGATATT
nagP-D-F	AAAGGGGTTTTAACTAAGATAAGCCCCTTCTGAGGAAG
nagP-D-R	GCGTCGGGCGATATCGAGGCGGACGAATACTTTGAC
GamP-U-F	GGTACCCGGGAGCTCTAGGGTAAAACCGTATGCCGC
GamP-U-R	AAGCAACTTCAGTTTTCCGGCATTCTCCTTATGTCAA
GamP-D-F	AAGGAGAATGCCGGAAAACTGAAGTTGCTTTTGAGGAATC
GamP-D-R	GCGTCGGGCGATATCGGAAATTTCTCTGCCAGCTGC
GamA-U-F	GGTACCCGGGAGCTCGGTCAAGAGGGAGGGTTCACTT
GamA-U-R	TGTCAGTCATTCAATGTTTTTCTCCTTTCCACAAAATAAA
GamA-D-F	GGAAAGGAGAAAAACATTGAATGACTGACAAAATCGGTTA
GamA-D-R	GCGTCGGGCGATATCTCATATCGGGGATCGGCTT
nagAB-U-F	GGTACCCGGGAGCTCCCGCACGGTCAGCTTA
nagAB-U-R	GGGAATCTTTTTTGATACAACTCTAGTTGTCTAGACCAAT
nagAB-D-F	ACAACTAGAGTTGTATCAAAAAAGATTCCCACATT
nagAB-D-R	GCGTCGGGCGATATCCCTCTTCATATCAATGACGAA
alsSD-U-F	GGTACCCGGGAGCTCAATTCGCTTGGCATTCCG
alsSD-U-R	GGAGGAGTGAGGGCTATGAAAAAGCCCTCTTTGAAAAG
alsSD-D-F	AGAGGGCTTTTTCATAGCCCTCACTCCTCCATTTTC
alsSD-D-R	GCGTCGGGCGATATCTGGGGATAAATCCGGCTTT
*Bl*glmS-U-F	GGTACCCGGGAGCTCCAGAAGACTGAAGAACGAGACA
*Bl*glmS-U-R	AATAGGCGTCACCTTAATTTTCTTCCTCCTAAAGTCG
P_{als}-glmS-F	AGGAGGAAGAAAATTAAGGTGACGCCTATTTCACT
P_{als}-glmS-R	TACAATACCACACATAGCCCTCACTCCTCCATT
*Bl*glmS-D-F	GGAGGAGTGAGGGCTATGTGTGGTATTGTAGGTTATATTG
*Bl*glmS-D-R	GCGTCGGGCGATATCTAATGCAATCGCATAAGAGC
pKVM-GamP-UP-F	CCTCGCGTCGGGCGATATCGGATCCTAGGGTAAAACCGTAT GCCGC
P_{als}-GamP-UP-R	AATAGGCGTCACCTTTCCGGCATTCTCCTTATGTCAA
Mt-GamP-UP-F	AACAGCAGCCAGTAAAAACTGAAGTTGCTTTTGAGGAATC
Ct-GamP-UP-F	AACAGCACGCAGTAAAAACTGAAGTTGCTTTTGAGGAATC
Nf-GamP-UP-F	AAACTGGCGTTTTAAAAACTGAAGTTGCTTTTGAGGAATC
Tt-GamP-UP-F	TATTATCATAAATAAAAACTGAAGTTGCTTTTGAGGAATC
pKVM-GamP-Down-R	CCATGGTACCCGGGAGCTCGAATTCGGAAATTTCTCTGCCA GCTGC
GamP-Up-P_{als}-F	AAGGAGAATGCCGGAAAGGTGACGCCTATTTCACTTTC
GamP-Down-Mt-R	AAGCAACTTCAGTTTTTACTGGCTGCTGTTGCTTTTC
GamP-Down-Nf-R	AAGCAACTTCAGTTTTTAAAACGCCAGTTTCATCTGC
GamP-Down-Ct-R	AAGCAACTTCAGTTTTTACTGCGTGCTGTTGCTTTT
GamP-Down-Tt-R	AAGCAACTTCAGTTTTTATTTATGATAATAATGCGCCATTT

References:

1. Deng MD, Severson DK, Grund AD, Wassink SL, Burlingame RP, Berry A, Running JA, Kunesh CA, Song L, Jerrell TA, Rosson RA. 2005. Metabolic engineering of *Escherichia coli* for industrial production of glucosamine and *N*-acetylglucosamine. Metab. Eng. *7*, 201–214.
2. Lee, S.W., Lee, B.Y., and Oh, M.K. (2018). Combination of three methods to reduce Glucose metabolic rate for improving *N*-acetylglucosamine production in *Saccharomyces cerevisiae*. J. Agric. Food Chem. *66*, 13191–13198.
3. Niu T, Lv X, Liu Y, Li J, Du G, Ledesma-Amaro R, Liu L. (2021). The elucidation of phosphosugar stress response in *Bacillus subtilis* guides strain engineering for high *N*-acetylglucosamine production. Biotechnol. Bioeng. *118*, 383–396.
4. Deng, C., Lv, X., Li, J., Zhang, H., Liu, Y., Du, G., Amaro, R.L., and Liu, L. (2021). Synergistic improvement of *N*-acetylglucosamine production by engineering transcription factors and balancing redox cofactors. Metab. Eng. *67*, 330–346.